Reports

World Ocean Tides Synthesized from Normal Modes

Abstract. *Sixty oceanic normal modes are used to synthesize the* M_2 *and* K_1 *(principal lunar semidiurnal and declinational diurnal) tides. The ten most energetic modes in the* M_2 *synthesis account for 87 percent of the energy; the corresponding figure for* K_1 *is 93 percent, two-thirds of which is contributed by a single mode whose natural period is about 29 hours. Model calculations indicate that the quality* (Q) *of the ocean response to tidal forcing resembles that of a frictionally controlled oscillator. In particular, for* M_2 *the global* Q *is about 10.*

Ocean-tide theorists have lately made significant improvements in numerical modeling of the global tide (*1*). Resolution of 1 degree in latitude and longitude is now computationally feasible, as is inclusion of the small but not negligible effect of tidal deformation of the solid earth. Probably the chief remaining model uncertainty arises from dissipation of tidal energy, whose mechanism has long resisted both physical and observational insight (*2*). Fortunately, however, the orbital history of the moon provides the crucial constraint that, whatever may be the details, dissipation by the M_2 tide should not exceed about 3.1×10^{12} W (*3*).

The almost periodic force that raises the tide varies smoothly in both latitude and longitude. If all of the ocean's natural frequencies were much higher than those of the force, the shape of the tidal deformation of the sea surface would closely resemble that of the force potential. For example, the amplitude of M_2 (principal lunar semidiurnal tide, period 12.42 hours) would have a peak of about 20 cm at the equator and would decline poleward like $\cos^2$(latitude), while the phase would increase linearly westward at the earth-rotation rate of 1 hour (strictly 1 lunar hour) in 15 degrees of longitude.

The actual (or numerically modeled) M_2 tide is strikingly different. It has a complexity of structure that must be ascribed to excitation of similarly complex free modes of vibration. The implied influential role of resonance has been accepted in varying degrees throughout the 200-year history of the theory of ocean tides, and is supported by numerous investigations of idealized models of the free modes (*4*). Computers now make it possible to extend these investigations to realistic ocean basins (*5*) and to create a catalog of the normal modes associated with a given tide model, taking full account of bathymetric details. (There has been an analogous development in models used for numerical weather prediction.)

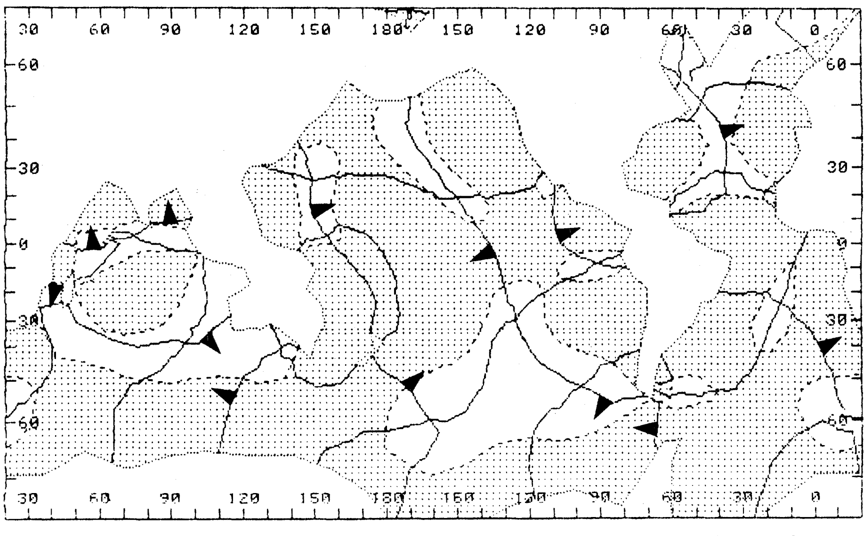

Fig. 1. Synthesized dynamical M_2 tide. The map is shaded where the amplitude of the sea-surface elevation exceeds 15 cm. Solid lines are isochrones of phase at intervals of 90° (three lunar hours). Zero phase coincides with the transit of the moon at Greenwich and is identified by an arrowhead pointing in the direction of propagation.

Figure 1 illustrates a further step in this direction. It is a map of the M_2 tide synthesized as a linear combination of normal modes. Each mode contributes to the synthesis to an extent determined by proximity of its frequency to that of the tide and by its spatial coherence with the tide potential. The map shown here was obtained from 60 modes with periods between 8 and 96 hours. Except for the dubious anticyclonic subtropical amphidrome in the North Atlantic and absence of the California amphidrome, it agrees qualitatively in most respects with maps derived by direct integration of Laplace's tidal equations. Although some details, such as the phase distribution near amphidromic centers, depend on the more weakly excited modes, 87 percent of the energy of the synthesized M_2 tide is supplied by only ten modes. If we restrict our view to an individual ocean region, such as the North Atlantic, an even smaller number of modes suffices to account for the main oceanic-scale features of the tide. In a rough way these results demonstrate the quasi-resonant quality of the ocean response to tidal excitation.

Spatial coherences between tide potential and principal modes are not large but neither are they pathologically small. As a measure of coherence one can use the coefficient of correlation between the sea-surface configuration of the potential and that of a particular mode, the square of which is equal to the normalized spectral density in modal decomposition of the potential. I find that the distribution of spectral density over mode frequency (Fig. 2) has a peak of about 0.1 near 0.8 cycle per day (period 30 hours) for both semidiurnal and diurnal potentials (respectively P_2^2 and P_2^1 surface spherical harmonics). Modes at that frequency have the largest geographic scale; this promotes coherence with the even larger-scale potential. On the high-frequency side of the peak the mode scale decreases with increasing frequency, in much the same way as for a vibrating membrane, and there is a corresponding loss of coherence with the potential. On the low-frequency side, where the modes are dominated by Coriolis force rather than gravity, the scale (and consequently the coherence) increases with increasing frequency.

The ten most energetic modes in the synthesized M_2 tide are in the frequency

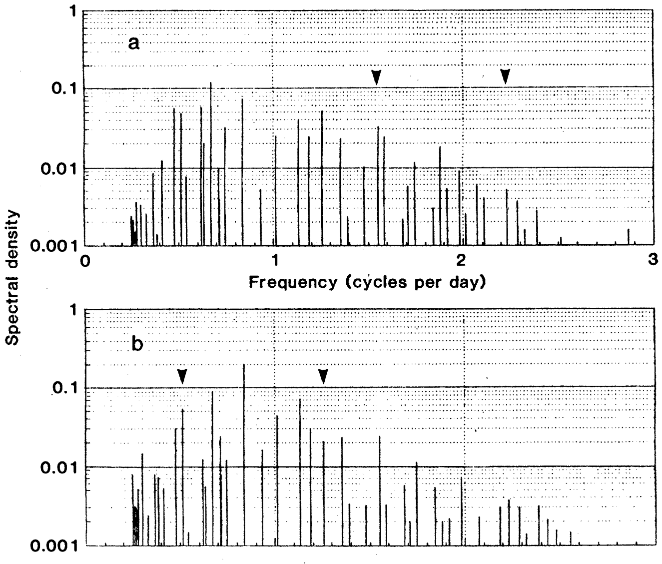

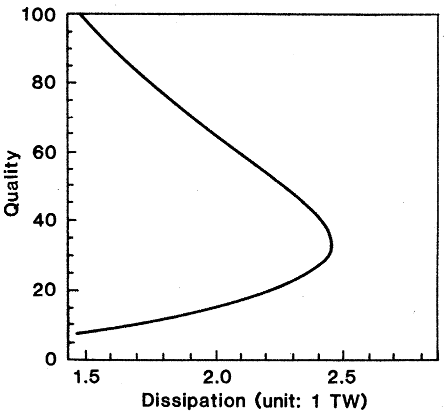

Fig. 2 (left). Normalized spectral densities in the mode decompositions of (a) the P_2^2 and (b) the P_2^1 spherical surface harmonics, corresponding, respectively, to the semidiurnal and diurnal tide potentials. Arrowheads indicate limits of frequency bands that contain the ten most energetic modes in syntheses of the M_2 and K_1 tides in (a) and (b), respectively. Fig. 3 (right). Quality (Q) of M_2 response, versus radiational dissipation. Increasing the effective shelf depth decreases Q. It also increases energy loss through the boundary, if the response is inertially controlled (high Q). When the shelf depth exceeds a critical value (in this model about 2.5 m), the response becomes frictionally controlled (low Q) and energy loss decreases with increasing shelf depth.

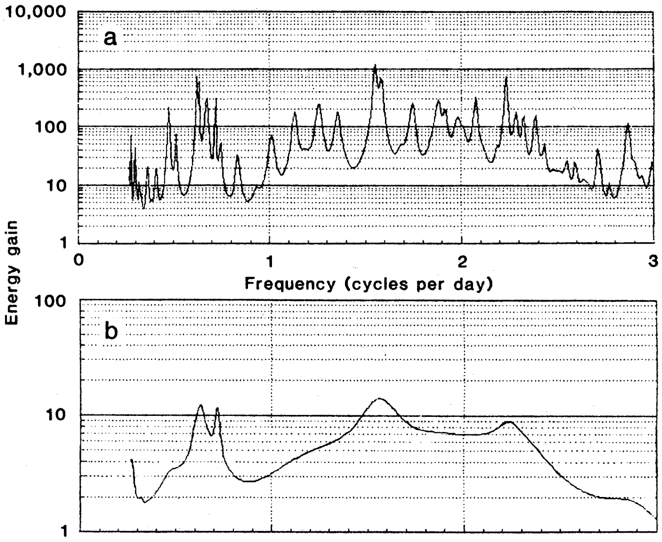

Fig. 4. Energy gain (ratio of synthesized-tide energy to equilibrium-tide energy) in response of the ocean to forcing by the P_2^2 potential over a continuous range of frequencies. The response in (a) was obtained with effective shelf depth 0.3 m and evidently is inertially controlled. In (b), with shelf depth 50 m, it is frictionally controlled. At the M_2 frequency (1.93 cycles per day), Q = 86 in (a) and 10 in (b).

band indicated by arrows in Fig. 2a. The average spectral density of these modes in the tide potential is about 0.0062 (*6*). In the synthesis of K_1 (declinational diurnal tide, period 23.93 hours), the ten most energetic modes (between arrows in Fig. 2b) provide 93 percent of the total energy and have an average spectral density of 0.056. It is remarkable that in K_1 the most energetic mode (period 28.7 hours, a combined fundamental basin oscillation of the Pacific and fundamental Kelvin wave of Antarctica) alone accounts for 61 percent of the total energy. In contrast, the synthesized M_2 tide has only 19 percent of its energy in the most energetic mode (period 12.8 hours, dominant in the South Atlantic).

The modes thus far used for tide synthesis are not dissipative, nor do they provide for self-attraction or crustal yielding. I have not yet attempted to overcome the latter limitations, but have applied standard variational analysis to introduce dissipation as a perturbation (*7*), and adopted a radiation boundary condition for that purpose (*8*). This condition is appropriate when the mesh size of the model does not give adequate resolution of direct frictional dissipation on continental shelves and in marginal seas, where most of the tidal energy loss is generally believed to be located. It introduces an ad hoc dissipation parameter, which can be fixed by specifying the depth of the energy-absorbing shelves. The tides described here were synthesized from a model with an effective shelf depth of 50 m. They do not provide for ocean-tide self-attraction or load-tide attraction and displacement, but were adjusted for earth-tide attraction and displacement by means of the Love reduction factor 0.69. On this basis, dissipation of the synthesized M_2 was found to be 1.7 TW (1 TW = 10^{12} W), considerably less than the astronomically derived 3.1 TW but not so much smaller than values from the most recent tide models (*9*).

Dependence of response energy on the dissipation parameter resembles the behavior of a damped harmonic oscillator. In particular, when expressed as a relation between dissipation D and response quality $Q = \omega E/D$ (where ω is tide frequency and E average stored energy), it exhibits a duality that permits both a high-Q and a low-Q response to have the same D (Fig. 3). An important feature of this duality is existence of a maximum possible dissipation, which in the present model is about 2.5 TW. This occurs at Q = 33 and for a shelf depth of 2.5 m. With D = 1.7 TW the two values of Q for the synthesized M_2 tide are about 86 (shelf depth 0.3 m) and about 10 (shelf depth 50 m) (*10*). By examining the corresponding maps of sea-surface elevation I found no difficulty in selecting the low-Q response ($E = 1.20 \times 10^{17}$ J) as the appropriate one: at Q = 86 the response is much too energetic. Moreover, at high Q the dependence of response energy on excitation frequency shows a conspicuous resonance peak at every mode, whereas at low Q it conforms to the "credo of smoothness" (*11*) (Fig. 4).

Unsatisfactory aspects of this work are the use of nondissipative modes and omission of ocean attraction and loading. To remedy these defects calls for greater computational effort.

GEORGE W. PLATZMAN
Department of the Geophysical Sciences, University of Chicago, Chicago, Illinois 60637

References and Notes

1. R. G. Gordeev, B. A. Kagan, E. V. Polyakov, *J. Phys. Oceanogr.* 7, 161 (1977); W. Zahel, *Ann. Geophys.* **33**, 31 (1977); Y. Accad and C. L. Pekeris, *Philos. Trans. R. Soc. London Ser. A* **290**, 235 (1978); M. E. Parke and M. C. Hendershott, *Mar. Geod.* **3**, 379 (1980); E. W. Schwi-

derski, *Rev. Geophys. Space Phys.* **18**, 243 (1980).

2. A new observational impetus was given by D. E. Cartwright, A. C. Edden, R. Spencer, J. M. Vassie [*Philos. Trans. R. Soc. London Ser. A* **298**, 87 (1980)] by means of a network of deep-sea bottom-pressure gages. Also encouraging are recent analyses of dissipation by V. Y. Gotlib and B. A. Kagan [*Dtsch. Hydrogr. Z.* **35**, 1 (1982)] and by E. W. Schwiderski (*Mar. Geod.*, in press) from numerical models of M_2.
3. For a recent assessment, see K. Lambeck, *The Earth's Variable Rotation* (Cambridge Univ. Press, New York, 1980, section 10.5).
4. S. S. Hough, *Philos. Trans. R. Soc. London Ser. A* **191**, 139 (1898); M. S. Longuet-Higgins, *ibid.* **262**, 511 (1968).
5. G. W. Platzman, *Science* **178**, 156 (1972); *J. Phys. Oceanogr.* **2**, 117 (1972): *ibid.* **5**, 201 (1975); *ibid.* **8**, 323 (1978); V. Y. Gotlib and B. A. Kagan, *Dokl. Akad. Nauk SSSR* **251**, 710 (1980); G. W. Platzman, G. A. Curtis, K. S. Hansen, R. D. Slater, *J. Phys. Oceanogr.* **11**, 579 (1981); V. Y. Gotlib and B. A. Kagan, *Dtsch. Hydrogr. Z.* **35**, 45 (1982).
6. The only estimate I know is one made by C. J. R. Garrett and W. H. Munk [*Deep-Sea Res.* **18**, 493 (1971)] from the age of the tide. In a model with a single resonant mode they found a spectral density of 0.01. This is not far from the mean of 0.0062 cited in the text or the value of 0.02 for the most energetic contributor to the synthesis of M_2.
7. After discretization, Laplace's tidal equation for a constituent $\bar{X}$ of frequency ω is $(L' - \omega B)X' = L\bar{X}$. Here $\bar{X}$ is the equilibrium tide, B the inertia matrix, $L = -iA$ the nondissipative tidal operator, and $L' = L + iD$ the dissipative operator, where D is the dissipation matrix. Details of B, A, and D are given in the fourth paper cited in (5) above. We seek to approximate X' by a synthesis $\Sigma\, a_k X_k'$ with a small set of the eigenfunctions X_k' of L'. This narrow-band synthesis will not be an exact solution, so a residual remains when it is substituted for X' in the tidal equation. The coefficients a_k are fixed by requiring this residual to be orthogonal to each of the adjoint eigenfunctions Y_k that correspond to the selected X_k'. The well-known result is

$$a_k = (\sigma_k' - \omega)^{-1}\, Y_k{}^H\, L\, \bar{X} / Y_k{}^H B\, X_k'$$

If D is small in the sense that σ_k' and X_k' differ only slightly from the nondissipative σ_k and X_k obtained with $D = 0$, then standard perturbation theory leads to $\delta\sigma_k = i\, X_k{}^H\, D\, X_k$ and

$$\delta X_k = i \sum_{j \neq k} (\sigma_k - \sigma_j)^{-1}\, (X_j{}^H D\, X_k)\, X_j$$

while $\delta Y_k = \delta X_k$. By this means a dissipative synthesis can be approximated in terms of nondissipative modes.
8. This condition was suggested for tide models by J. Proudman [*Mon. Not. R. Astron. Soc. Geophys. Suppl.* **5**, 23 (1941)]. Its first use in a numerical model was by F. Gohin [*Proc. 7th Conf. Coastal Eng.* **2**, 485 (1961)] for M_2 in the North Atlantic. Y. Accad and C. L. Pekeris [cited in (*1*) above] applied a modified form of it in their model of M_2 and S_2 in the world ocean. Further modifications were examined by V. Y. Gotlib and B. A. Kagan [in (*2*)].
9. Y. Accad and C. L. Pekeris [in (*1*)], M. E. Parke and M. C. Hendershott [in (*1*)], V. Y. Gotlib and B. A. Kagan [in (*2*)], and E. W. Schwiderski [in (*2*)] find, respectively, 2.55, 2.22, 1.89, and 1.86 TW. These values are distinctly lower than the assessment of 3.35 TW by K. Lambeck [in (*3*), section 10.4] from earlier tide models, and point to the long-standing discrepancy between estimates of ocean-tide dissipation and inferences from the observed secular acceleration of the moon.
10. The Q values in recent numerical models of M_2 are: M. E. Parke and M. C. Hendershott [in (*1*)], Q = 17 (based on energy equipartition); V. Y. Gotlib and B. A. Kagan [in (*2*)], Q = 28 or 29 for three of their parameterizations of dissipation; E. W. Schwiderski [in (*2*)], Q = 10. I find the energy of the synthesized M_2 tide partitioned as 56 percent irrotational kinetic, 41 percent potential (in good agreement with Schwiderski's 42 percent), and 3 percent rotational kinetic.
11. W. H. Munk and D. E. Cartwright, *Philos. Trans. R. Soc. London Ser. A* **259**, 533 (1966); see *ibid.*, p. 544.
12. This material is based on work supported by NSF grant OCE-8110929. The manuscript was revised while I was a visitor at the National Center for Atmospheric Research.

22 November 1982; revised 15 February 1983

Phase Transition and Crystal Structure of the 37°C Form of Cholesterol

Abstract. *Crystalline cholesterol undergoes a phase transition a few degrees below human body temperature. The high-temperature form has an unusually complex structure with 16 independent molecules. In the transition two molecules change side chain conformation, four reorient about their long axes, and ten remain unchanged. The transition mechanism implies relatively nonspecific intermolecular interactions, qualitatively consistent with the behavior of cholesterol in biomembranes. The transition preserves a remarkably closely obeyed pseudosymmetry present in the structure.*

The reversible phase transition in crystalline anhydrous cholesterol, first reported in 1965, has been the subject of numerous studies by thermochemical, powder x-ray crystallographic, and nuclear magnetic resonance (NMR) methods (*1–4*). The transition temperature 31.60 ± 0.1°C was determined for single crystals of cholesterol (*3*); the transition enthalpy is 0.69 kcal/mole (*4*). In earlier studies the monohydrate was reported to be the only form present in biological deposits of crystalline cholesterol, such as gallstones and atherosclerotic plaques (*5*). Recently, however, the phase transition was detected in freshly removed human gallstones by means of differential scanning calorimetry (*4*). This indicates that the anhydrous form of cholesterol is present in gallstones in addition to the cholesterol monohydrate, which does not exhibit a transition. A suggested relation between the phase transition and the apparent dependence of atherosclerosis on species body temperature (*6, 7*) remains unsupported in the absence of evidence that the anhydrous form of cholesterol is present in atherosclerotic deposits.

The calorimetric and NMR data have been taken to indicate that the phase transition involves a change in the packing of the side chain methyl groups (*2*) or other rearrangement or onset of disorder in the side chains (*7, 8*). The strong influence of cholesterol content on the gel-liquid crystal phase transitions of lipid bilayers and membranes has been qualitatively ascribed to the lateral packing requirements of rigid steroid skeletons and flexible hydrocarbon chains (*9–12*). To our knowledge, no crystals have yet been prepared of mixed (or stoichiometric, if such exist) phospholipid-cholesterol systems, but the packing of steroid nuclei by themselves and with interdigitating hydrocarbon chains in crystals of cholesterol derivatives has been considered a possible model for biological bilayers (*13*).

Crystals of the body-temperature form grown from 1,4-dioxane solution by slow evaporation at 37°C were mounted, transferred, and examined on the diffractometer while maintained at 37° ± 1°C. Data were collected to a resolution of 0.97 Å (deviation of diffracted beam from direct beam = $2\theta \leq 105°$). The crystals belong to the triclinic space group $P1$ and have a remarkably large unit cell containing 16 independent cholesterol molecules, compared to 8 in the room-temperature (25°C) cell (*14*). The 37°C cell is formed from the 25°C cell by a doubling of the **a** axis. Lattice parameters are given in Table 1.

The structure solution was initiated with an assumed model consisting of two copies of the 25°C structure placed in the 37°C cell and translated by **a**/2 relative to one another. This model was first refined against data for only even values of the index h, using a restrained rigid-body refinement program employing the Gauss-Seidel least-squares algorithm, in which the calculated structure factors are updated after each shift of a rigid group of atoms (*15*). The refinement resulted in considerable rotation of several molecules about their long axes.

Table 1. Comparison of unit cell parameters (*19*) of cholesterol above and below the 31.6°C phase transition.

Temperature (°C)	Unit cell axes (Å)			Unit cell angles (deg)			Z	ρ (g cm^{-3})
	a	**b**	**c**	α	β	γ		
37*	27.565(10)	35.776(16)	10.748(4)	94.45(3)	90.90(3)	73.87(3)	16	1.012
37†	27.565(10)	34.594(15)	10.748(4)	94.25(3)	90.90(3)	96.55(3)	16	1.012
25‡	14.172 (7)	34.209(18)	10.481(5)	94.64(4)	90.67(4)	96.32(4)	8	1.021

*Reduced 37°C cell, whose lattice parameters are related to the reduced 25°C cell by the approximate relations $\mathbf{a}_{37} \simeq 2\mathbf{a}_{25}$, $\mathbf{b}_{37} \simeq \mathbf{a}_{25} + \mathbf{b}_{25}$, and $\mathbf{c}_{37} \simeq \mathbf{c}_{25}$. †Nonstandard 37°C cell, used in Fig. 1, related to the 25°C cell by an approximate doubling of **a**. ‡Reduced 25°C cell (*14*) shown for comparison.